A Requirement for Bid for Induction of Apoptosis by Photodynamic Therapy with a Lysosome- but not a Mitochondrion-Targeted Photosensitizer

Song-mao Chiu[1], **Liang-yan Xue**[1], **Minh Lam**[2,4], **Myriam E. Rodriguez**[2], **Ping Zhang**[3], **Malcolm E. Kenney**[3,4], **Anna-Liisa Nieminen**[5,6], and **Nancy L. Oleinick**[1,4]

[1]Department of Radiation Oncology, Case Western Reserve University, Cleveland, OH 44106, USA

[2]Department of Dermatology, Case Western Reserve University, Cleveland, OH 44106, USA

[3]Department of Chemistry, Case Western Reserve University, Cleveland, OH 44106, USA

[4]The Case Comprehensive Cancer Center, Case Western Reserve University, Cleveland, OH 44106, USA

[5]Department of Pharmaceutical and Biomedical Sciences, Medical University of South Carolina, Charleston, SC 29425, USA

[6]The Hollings Cancer Center, Medical University of South Carolina, Charleston, SC 29425, USA

Abstract

Photodynamic therapy (PDT) with lysosome-targeted photosensitizers induces the intrinsic pathway of apoptosis via the cleavage and activation of the BH3-only protein Bid by proteolytic enzymes released from photo-disrupted lysosomes. To investigate the role of Bid in apoptosis induction and the role of damaged lysosomes on cell killing by lysosome-targeted PDT, we compared the responses of wild type and Bid-knock-out murine embryonic fibroblasts toward a mitochondrion/endoplasmic reticulum-binding photosensitizer, Pc 4, and a lysosome-targeted sensitizer, Pc 181. Whereas apoptosis and overall cell killing were induced equally well by Pc 4-PDT in both cell lines, Bid$^{-/-}$ cells were relatively resistant to induction of apoptosis and to overall killing following PDT with Pc 181, particularly at low PDT doses. Thus, Bid is critical for the induction of apoptosis caused by PDT with the lysosome-specific sensitizers, but dispensable for PDT targeted to other membranes.

INTRODUCTION

Photodynamic therapy (PDT) kills cells via singlet oxygen and other reactive oxygen species that are generated following visible light activation of non-toxic photosensitizers in the presence of molecular oxygen (1,2). Because of the high reactivity of these oxygen products, initial subcellular damage occurs at sites where the photosensitizers accumulate (3). Numerous photosensitizers have been developed that preferentially target one or more cellular components, such as plasma membrane, mitochondria, endoplasmic reticulum (ER), or lysosomes. Depending on the cell type, type of photosensitizer, and dose of PDT, PDT may induce apoptotic or nonapoptotic cell death; the latter includes necrosis and autophagy

---

(4,5). PDT with photosensitizers that selectively accumulate in mitochondria and ER causes photodamage to the anti-apoptotic proteins Bcl-2 and Bcl-xL and induces the intrinsic pathway of apoptosis, which proceeds via Bax activation, release of cytochrome c from mitochondria to cytosol, and activation of caspases, resulting in cell shrinkage and chromatin condensation and fragmentation (4) .

Kessel and Reiners and their colleagues (6) showed that PDT sensitized by N-aspartyl chlorin e6 (NPe6) damages lysosomes. In a subsequent study, they demonstrated that NPe6 accumulates in lysosomes and initiates the mitochondrial pathway of apoptosis, as evidenced by cleavage of the BH3-only protein Bid, the release of cytochrome c from mitochondria and activation of procaspases-9 and −3 (7). In this case, the kinetics of apoptosis development were slower than for mitochondrion-targeted PDT, and Bid was cleaved at the time of cytochrome c release, presumably by proteases released from lysosomes. It was hypothesized that the mitochondrial pathway is triggered by truncated Bid (t-Bid), an active form of Bid. Bid has an important role in the cross-talk between the extrinsic and intrinsic pathways of apoptosis (8), in that when cleaved and activated by caspase-8, it is able to induce mitochondrial outer membrane permeabilization resulting in cytochrome c release from mitochondria (9,10). However, proteases of lysosomal extracts differ from death receptor-activated caspase-8 in their cleavage sites on the Bid protein and in their inability to directly cleave and activate procaspases to initiate a caspase cascade by a Bid-independent pathway (11). Similar apoptosis induction has been reported recently following PDT with another lysosome-targeting photosensitizer, ATX-S10 (12). Subsequently, Wan et al. (13) studied NPe6-sensitized PDT in human lung adenocarcinoma (ASTC-a-1) cells and demonstrated that knockdown of Bid by shRNA made the cells relatively resistant to PDT. Using the loss of fluorescence resonance energy transfer (FRET) in overexpressed YFP-Bid-CFP as a measure of Bid cleavage, they also showed that Bid cleavage was dependent on cathepsins but not on caspase-8. However, it is unclear how important the Bid-mediated amplification of the mitochondrial pathway is for other lysosome-localizing photosensitizers.

We have been studying PDT with the phthalocyanine photosensitizer Pc 4 for a number of years. Pc 4 localizes preferentially to mitochondria and the ER in a range of human cancer cells and upon photoirradiation efficiently induces the intrinsic pathway of apoptosis (reviewed in (4)). We recently reported a study of a series of Pc 4 analogues that preferentially bind to lysosomes; Pc 181 is representative of this group of photosensitizers. In comparison to Pc 4, Pc 181 was taken up into human breast cancer MCF-7 cells more efficiently and produced greater photodynamic cell killing, as judged by a colony-formation assay (14). However, induction of apoptosis by Pc 181-PDT was delayed and considerably less efficient than by Pc 4-PDT. To elucidate the effect of lysosomal photodamage on cell killing as well as to gain further insight into the role of Bid in the induction of the mitochondrial pathway of apoptosis following lysosome-targeted PDT, we have compared Pc 4 and Pc 181 with respect to their ability to induce apoptosis and cell killing in PDT protocols in normal wild-type (Bid$^{+/+}$) and Bid knock-out (Bid$^{−/−}$) murine embryonic fibroblasts (MEFs). Our data indicate that Bid is required for cell death in the case of lysosome- but not mitochondrion-targeted PDT and further that MEFs become relatively resistant to lysosome-targeted PDT in the absence of Bid.

MATERIALS AND METHODS

Cell culture

Immortalized murine embryonic fibroblasts (MEFs) from wild-type (Bid$^{+/+}$) and Bid knock-out (Bid$^{−/−}$) mice were obtained from Atan Gross (Department of Biological Regulation, Weizmann Institute of Science, Rehovot, Israel). MEFs were grown in Dulbecco's Modified

Eagle's Medium (DMEM) supplemented with 10% fetal bovine serum, 2 mM L-glutamine, and antibiotics in a humidified 37°C incubator in an atmosphere of 5% CO_2 in air.

Photodynamic treatments

The phthalocyanine photosensitizers Pc 4 [HOSiPcOSi- $(CH_3)_2(CH_2)_3N(CH_3)_2$] and Pc 181 [SiPc(OSi$(CH_3)_2(CH_2)_3N(CH_3)_2$)(OSi$(CH_3)_2(CH_2)_4$-CHOHCH$_2$OH)] (Fig. 1) were synthesized as previously described (14) and used as 0.5 mM stock solutions in dimethyl formamide. An aliquot of Pc 4 or Pc 181 diluted in culture medium was loaded to the monolayer cell cultures to give a final concentration of 0–300 nM 16–18 h before exposure of the cultures to 200 mJ/cm^2 red light at 1.0 mW/cm^2. The light source was a light-emitting diode array (EFOS, Mississauga, Ontario, Canada) delivering narrow band light (λ_{max}, 670–675 nm; 24 nm width at half maximum) centering on the main absorption peak of the photosensitizers (λmax ~672 nm in biological medium). Irradiation was carried out at room temperature and was followed by incubation of the cultures in the dark at 37°C for various periods of time before harvest.

Confocal microscopy

Cells were cultured in 35-mm glass-bottomed tissue culture dishes (MatTek Corporation, Ashland, MA) at 1×10^5 cells per dish. The cultures were incubated in either 200–300 nM Pc 4 or 40–100 nM Pc 181 for 18 h and either 30 min in 100 nM MitoTracker Green (MTG) or overnight in 0.2 mg/mL Oregon Green Dextran (OGD). Both dyes were purchased from Invitrogen (Carlsbad, CA). Images were acquired using a 63× N.A. 1.4 oil immersion planapochromat objective on a Zeiss LSM 510 confocal microscope in the Case Comprehensive Cancer Center Confocal Microscopy Core Facility. Confocal images of Pc 4 and Pc 181 fluorescence were collected using a 633-nm excitation light supplied by a helium/neon laser, a 633-nm dichroic mirror, and a 650-nm long-pass filter. Images of MTG or OGD were collected using a 488-nm excitation light from the argon laser, a 488-nm dichroic mirror, and a 500–550 nm band-pass barrier filter.

Cellular uptake of Pc 181

The quantification of photosensitizer uptake was conducted essentially as described (13). Briefly, exponentially growing cultures in 60-mm culture dishes were incubated with various concentrations of Pc 181 for 18 h. The cells were harvested by trypsinization, washed once, suspended in PBS, and then subjected to flow cytometric analysis with an EPICS Elite Flow Cytometer (Flow Cytometiry Core Facility, Case Comprehensive Cancer Center). Pc 181 was excited by a broadband UV laser (335–365 nm), and fluorescence emission was collected with a 650-nm long-pass filter.

Percentage of cells with less than the G1 content of DNA

Detached cells together with cells collected by trypsinization were fixed with formaldehyde, permeabilized, and stained with propidium iodide (PI), as described (15). The stained samples were analyzed by flow cytometry as above, with λex = 488 ± 20 nm and λem = 620 ± 20 nm..

Determination of cell viability

Two methods were used to monitor cell viability. For the trypan blue exclusion assay, cells were stained with 0.2% trypan blue and examined by light microscopy. Alternatively, cell viability was measured using the tetrazolium salt MTT (3- [4,5-dimethylthiazol-2-yl]-2,5 diphenyl-tetrazolium bromide, Sigma), essentially as described (16). Cells were seeded into 96-well plates and allowed to attach and grow overnight. Following exposure to PDT as described above and 22 h post-irradiation incubation, they were subjected to MTT assay.

Assessment of cytochrome c release from mitochondria

The release of cytochrome c from mitochondria to cytosol was assessed by immunohistochemical staining as described (15,17). Briefly, formaldehyde-fixed cells were incubated with mouse anti-cytochrome c (1: 200 dilution, cat. No. 556432, BD Pharmingen, San Diego, CA) and then with Hoechst 33342 and the second antibody, which was anti-mouse IgG conjugated to Texas red (Vector Laboratories, Burlingame, CA). The cover slips were mounted on slides and examined with an inverted Olympus fluorescence microscope. Images were photographed with a Spot RT digital camera.

Fluorescence microscopy of nuclei, mitochondria and lysosomes

For nuclear morphology, cells grown on coverslips were fixed in PBS containing 3.7% formaldehyde, stained with 5 µg/mL Hoechst 33342 (HO, Invitrogen, Carlsbad, CA), and examined by fluorescence microscopy. Apoptotic cells were identified by the characteristic features of their nuclei: chromatin condensation, margination and fragmentation. At least 200 cells were counted from each sample, and the yield of apoptotic cells was expressed as a percentage of the total population. Since detached cells, which are enriched in apoptotic cells, were not included in this measurement, the estimated percentage of apoptosis determined here is a minimum. For imaging lysosomes, the cultures were loaded with 1 µg/mL of acridine orange (AO) for 20 min. Changes in mitochondrial membrane potential ($\Delta\Psi_m$) were monitored by the uptake of JC-1, as previously described (15). JC-1 [5,5',6,6'-tetrachloro-1,1',3,3'-tetraethyl-benzimidazolyl-carbocyanine iodide] was supplied by Molecular Probes (Eugene. OR) and dissolved in DMSO to produce a 1 mg/mL stock solution. Cells were incubated at 37°C in culture medium containing 10 µg/mL JC-1 for 30 min 2–5 h after PDT. Samples were washed once with PBS and examined for red-orange fluorescence.

Western blot analysis

Cells were lysed, sonicated, and boiled in protein gel buffer (50 mM Tris-HCl, pH 6.8, 1% SDS, 1% mercaptoethanol, and 5% glycerol). 20 µg of cellular protein as measured using the BCA protein assay reagent (Pierce Chemical, Rockford, IL) were analyzed on 12% SDS-PAGE gels. After transfer to PVDF membranes, the proteins were probed with one or more of the following antibodies: anti-Bax (1:500 dilution, cat no. N-20, Santa Cruz, Santa Cruz, CA), anti-Bak (1:1000 dilution, cat no.06536, Millipore, Billerica, MA), anti-Bid (1:500 dilution, cat. no. 550365, BD Biosciences, San Diego, CA), anti-active caspase-3 (1:1000 dilution, cat. No. 559565, BD Pharmingen, San Diego, CA) or anti-actin (1:2000 dilution, cat.no. MS-1295, NeoMarker, Fremont, CA). They were then incubated with peroxidase-conjugated second antibodies, and the immune complexes were detected by enhanced chemiluminescence system (Amersham, Arlington Heights, IL).

RESULTS

Localization of Pc 181 to lysosomes of MEFs

Our laboratory has shown that the photosensitizer Pc 4 accumulates in intracellular membranes, especially those of mitochondria and ER, of human carcinoma cells (18,19,20). The recently developed analogue Pc 181, in contrast, has been found to accumulate almost exclusively in the lysosomes of human breast cancer MCF-7 cells (14). Consistent with those findings, MEFs loaded with Pc 4 displayed an extranuclear pattern of fluorescence and partially co-localized with the mitochondrion-specific dye MTG, indicated by the orange-yellow color in the merged image of red Pc 4 and green MTG (Fig. 2A). As expected, Pc 4 did not co-localize with the punctate pattern defined by the lysosome-specific OGD (Fig. 2B). In contrast, the fluorescence image of Pc 181 was decidedly different from that of

MTG, and it did not co-localize with this dye (Fig. 2C). Instead, the fluorescence image of Pc 181 was punctate and perinuclear similar to that of OGD, with which it partially co-localized (Fig. 2D). There was no significant difference in the Pc 4 and Pc 181 fluorescence images in Bid$^{+/+}$ vs. Bid$^{-/-}$ MEFs.

The absence of Bid makes MEFs more resistant to PDT with Pc 181 but not Pc 4

Bid$^{+/+}$ and Bid$^{-/-}$ MEFs were compared for their sensitivity to PDT. The presence and absence of Bid protein in Bid$^{+/+}$ and Bid$^{-/-}$ cells, respectively, were confirmed on western blots (Fig. 3). Probing of the blots with antibodies against the apoptotic effectors Bax and Bak revealed the presence of approximately similar levels of these proteins in the two MEF lines.

When MEFs were exposed to PDT with Pc 4 or Pc 181 and analyzed for cell viability by the MTT assay, Bid$^{+/+}$ and Bid$^{-/-}$ cells were found to be equally sensitive to Pc 4-PDT, whereas Bid$^{-/-}$ MEFs were relatively resistant to killing by Pc 181-PDT, especially at Pc 181 concentrations of 20 and 40 nM (Fig. 4A,B). At higher doses of PDT, Bid$^{-/-}$ cells remained more resistant than Bid$^{+/+}$ MEFs, although the difference in sensitivity was statistically significant only for concentrations of Pc 181 below 80 nM. The relative resistance of Bid$^{-/-}$ MEFs toward killing by Pc 181-PDT was also observed by trypan blue exclusion, but not at concentrations above 100 nM, which reduced viability to less than 10% (Fig. 4C). Interestingly, the presence of a shoulder on the dose-response curve in the Bid$^{-/-}$ cells shifts the curve to the right of that for Bid$^{+/+}$ cells, but the slopes of the dose-response curves for the two MEF lines above 40 nM Pc 181 are essentially identical.. A comparison of the MTT data for the two lines (Fig. 4A,B) also shows that Pc 181-PDT is more potent than Pc 4-PDT in the presence of Bid, with 50% toxicity requiring approximately 100 nM Pc 4 but only 60 nM Pc 181. In the absence of Bid, the LD50 dose was 100 nM of either photosensitizer. In MCF-7c3 cells, which express Bid, a 4–6-fold lower concentration of Pc 181 than Pc 4 was sufficient to achieve equal cytotoxicity (14). For the following mechanistic studies, we selected 100 nM Pc 181 because it produced a marked response yet a difference in sensitivity between the two cell lines could be discerned (Fig. 4B,C). For Pc 4-PDT, 100 nM or 300 nM were used, since the two lines were equally sensitive at all concentrations (Fig. 4A).

Bid$^{-/-}$ MEFs are more resistant than Bid$^{+/+}$ MEFs to the induction of apoptosis by Pc 181-PDT but are equally sensitive to Pc 4-PDT-induced apoptosis

Both Bid$^{+/+}$ and Bid$^{-/-}$ MEFs underwent morphological changes characteristic of apoptosis starting 2 h after exposure to an LD$_{95}$ dose of Pc 4-PDT (300 nM Pc 4 and 200 mJ/cm^2 red light). As displayed in Fig. 5A, almost all treated cells rounded up and detached from the monolayer by 24 h after PDT. Similar morphological changes occurred in Bid$^{+/+}$ MEFs after Pc 181-PDT. In contrast, only a small fraction of Bid$^{-/-}$ cells changed morphology after Pc 181-PDT (Fig. 5A).

We and others have found that PDT is an efficient inducer of apoptosis (4). Following Pc 4-PDT, equivalent levels of treated Bid$^{+/+}$ and Bid$^{-/-}$ MEFs displayed the nuclear apoptotic features of chromatin condensation and fragmentation.(Fig. 5B; 5C, right panel) or had a hypodiploid content of DNA (Fig. 5C, left panel), and the level of apoptosis increased with PDT dose in the range 100–300 nM Pc 4 (Fig. 5C). Similarly, PDT with Pc 181 also induced morphological apoptosis in both MEF lines, although the extent of apoptosis was much reduced in cells lacking Bid (Fig. 5B,D). For example, treatment of MEFs with 100 nM Pc 181 and 200 mJ/cm^2 red light resulted in about 50% of the Bid$^{+/+}$ cells but only 20% of the Bid$^{-/-}$ cells revealing nuclear apoptotic features (Fig. 5D, right panel) or a sub-G1 DNA

content (Fig. 5D, left panel). Higher doses of Pc 181-PDT, however, induced extensive apoptosis in both MEF lines (Fig. 5D).

Cell uptake of photosensitizers is an important determinant of photosensitivity (20). Therefore, we determined whether the difference in photosensitivity between $Bid^{+/+}$ and $Bid^{-/-}$ is due to a difference in the ability of the cells to internalize Pc 181. Uptake was assessed by flow cytometry. In Fig. 5E, the left panel shows an example of the histograms for 0 and 80 nM Pc 181 in each cell line, and the right panel is a summary of all uptake data. Uptake of Pc 181 was concentration dependent up to 200 nM but was not significantly different between the two cell lines. Therefore, the absence of Bid did not affect photosensitizer uptake, and the differential sensitivity of the cells cannot be attributed to different amounts of Pc 181 in them.

Retention of cytochrome c in mitochondria following Pc 181-PDT in $Bid^{-/-}$ MEFs

The release of cytochrome c from mitochondria into the cytosol following PDT, as reflected in changes in the immunofluorescence staining for cytochrome c from a punctate perinuclear pattern to a diffuse pattern, was observed in both MEF lines after Pc 4-PDT (Fig. 6A,B); it occurred as early as 6 h post-PDT after PDT with 300 nM Pc 4, but was found to be quite limited at 24 h after PDT with 100 nM Pc 4. This result was similar to changes observed with Pc 4-PDT in other cell lines (21,22). For Pc 181-PDT, a similar release of cytochrome c was found in $Bid^{+/+}$ cells (Fig. 6C), but not in the majority of $Bid^{-/-}$ cells (Fig. 6D). Time courses for the release of cytochrome c from mitochondria following PDT with 50 or 100 nM Pc 181 are presented in Fig. 6E. In $Bid^{+/+}$ cells, the release began as early as 1 h after the higher PDT dose and was near a maximum level within 3 h, whereas after the lower PDT dose, the release was considerably slower. In $Bid^{-/-}$ cells significant release did not occur until 3 h after the higher PDT dose and was not noticeably different from the controls up to 5 h after the lower PDT dose. Thus, cytochrome c release was more rapid and more extensive in the Bid-replete cells.

Bid cleavage following PDT

Bid is activated following cleavage by caspase-8 or other proteases (23). PDT with either Pc 4 or Pc 181 causes cleavage of Bid to a 15-kDa fragment (tBid) in MCF-7c3 cells (14). We found that treatment of $Bid^{+/+}$ MEFs with 50 or 100 nM Pc 181-PDT resulted in the production of tBid as early as 1 h after PDT (Fig. 7A); a lower dose (PDT with 40 nM Pc 181) required 3 h to reveal tBid (Fig. 7B). The level of tBid was lower at 5 h (Fig. 7A), because of extensive protein degradation resulting from fast induction of apoptosis in MEFs (14). In contrast, PDT with 50 nM Pc 4, which is approximately equitoxic to 40 nM Pc 181-PDT) produced no detectable Bid cleavage during the first 5 h after PDT (Fig. 7B). However, Bid cleavage was observed early after a higher dose of PDT (with 150 nM Pc 4) (Fig. 7B). The dose and time requirements to visualize the cleavage of Bid indicate that Pc 181-PDT is a more immediate activator of the requisite protease(s) than is Pc 4-PDT. However, it is not yet clear whether the cleavage is by caspase-8 at Asp[59] of Bid or by lysosomal proteases at Arg[65], as demonstrated by Stoka *et al*. (11). The SDS gels are not sufficiently sensitive to distinguish the two different cleavage products.

PDT with Pc 181 destroys lysosome integrity

Acridine orange is a lysosomotrophic and metachromatic fluorophore that once protonated is retained within acidic compartments, such as lysosomes, where it emits red fluorescence (7). When presented to untreated MEFs, AO is found as intense red fluorescent perinuclear spots (Fig. 8). Early (1 or 1.5 h) following PDT with 100 nM Pc 181, a drastic reduction in lysosomal AO was observed, and by 3.5 h almost all AO staining was abolished; this occurred in both $Bid^{+/+}$ and $Bid^{-/-}$ MEFs (Fig. 8A,B). A similar observation following PDT

with the lysosome-targeted photosensitizer NPe6 has been reported by Reiners *et al*. (7). These results indicate that the integrity of the lysosomes is destroyed by a lethal dose of Pc 181-PDT. In contrast, treatment of MEFs with a lower PDT dose (with 40 nM Pc 181) resulted in lighter but mostly punctate AO staining of lysosomes (Fig. 8), suggesting that most lysosomes remained intact for at least two h after the lower dose that was not lethal to $Bid^{-/-}$ MEFs (cf. Fig. 4).

Loss of mitochondrial membrane potential after PDT with Pc 181

Pc 4-PDT causes mitochondrial dysfunction within three hours after treatment in both MEF lines (data not shown), as reported previously for other cell lines (21,23). The effect of Pc 181-PDT on MEFs was monitored with JC-1, a cationic dye that is taken up into mitochondria with an intact mitochondrial membrane potential ($\Delta\psi_m$). As shown in Fig. 9, the uptake of JC-1 was virtually unaffected immediately after PDT, indicating that Pc 181-PDT did not cause direct photodamage to membranes of mitochondria. However, the majority of $Bid^{+/+}$ MEFs lost $\Delta\psi_m$ by 3.5 h after PDT (Fig. 9A), whereas $Bid^{-/-}$ MEFs retained substantial levels of $\Delta\psi_m$ at this time (Fig. 9B). Caspase-3 was strongly activated by 3 hours after Pc 181-PDT in $Bid^{+/+}$ MEFs (Fig. 9C).

DISCUSSION

The present study clearly indicates that $Bid^{+/+}$ and $Bid^{-/-}$ MEFs respond differently to Pc 4- and Pc 181-PDT. While the two cell lines are equally susceptible to Pc 4-PDT, the $Bid^{-/-}$ cells are resistant to low doses of Pc 181-PDT. Pc 181 is representative of Pc 4 analogues that contain two large axial siloxy ligands on the central silicon, one identical to that of Pc 4 and the other bearing one or more hydroxyl groups (14). Although Pc 4 and Pc 181 have the same Pc ring and one identical axial ligand, they preferentially target different subcellular compartments, mitochondria/ER and lysosomes, respectively. Therefore, the difference in sensitivity of the two cell lines toward PDT with these two photosensitizers likely reflects the difference in the mechanisms of cell killing caused by initial photodynamic damage in the different compartments. PDT with Pc 4 causes immediate photodamage to the anti-apoptotic proteins, Bcl-2 and Bcl-xL, in mitochondria and ER; the initial damage leads to activation of Bax and initiation of the intrinsic pathway of apoptosis and cell death (4). In MCF-7 cells, much less photodamage to Bcl-2 is found with Pc 181-PDT than with Pc 4-PDT at equitoxic doses (14), consistent with the differential targeting of the photosensitizers.

PDT with lysosome-targeting photosensitizers, including Pc 181, also induces the mitochondrial pathway of apoptosis, despite causing direct photodamage to lysosomes rather than mitochondria. According to Reiners *et al*. (7), triggering of the mitochondrial pathway following impairment of lysosomes is mediated by the cleavage and activation of Bid as a consequence of the release of proteases from lysosomes. With the lysosome-targeted NPe6 as photosensitizer, cathepsin-mediated Bid cleavage was also shown to be an integral part of the pathway from photodamage to mitochondrial apoptosis in human lung adenocarcinoma cells (13). Similar triggering of apoptosis by cathepsin-cleaved Bid following lysosome disruption has been reported in another (non-PDT) system (24). Our results with Pc 181-PDT support this conclusion and demonstrate that in the absence of Bid, the link between lysosome photodamage and activation of the intrinsic pathway of apoptosis is broken, and as a consequence the downstream events, such as the release of cytochrome c from mitochondria and the development of nuclear apoptosis, are blocked. Since neither apoptosis induction nor overall photocytotoxicity of MEFs is compromised in the absence of Bid following Pc 4-PDT, Bid must not be involved in Pc 4-PDT, even though it is cleaved less extensively and late in the process, presumably via caspases activated by PDT or from non-specific binding of Pc 4 to lysosomes at the higher concentrations.

The Pc 181-PDT dose-survival curves of Bid$^{+/+}$ and Bid$^{-/-}$ MEFs (Fig. 4B) reveal aspects of the mechanism of cell killing. Bid$^{-/-}$ cells were almost completely resistant to PDT at Pc 181 concentrations of 20 and 40 nM, but at higher concentrations the survival curve paralleled that of the Bid$^{+/+}$ cells. Thus, the shoulder on the survival curve of the Bid$^{-/-}$ cells effectively shifts the curve to the right. The absence of significant differences between Bid$^{+/+}$ and Bid$^{-/-}$ cells in the cellular uptake of Pc 181 (Fig. 5E) or its subcellular localization (Fig. 2C,D), and the similar sensitivity of the two cell lines to loss of lysosomal integrity in response to Pc 181-PDT (Fig. 8) suggest that the block is not at the level of the initial photodamage to lysosomes. However, Bid$^{-/-}$ cells were less sensitive to apoptosis induction by Pc 181-PDT than were Bid$^{+/+}$ MEFs, as measured by cell morphology (Fig. 5A), nuclear morphology (Fig. 5B,D), flow cytometry (Fig. 5D), cytochrome c release (Fig. 6), and loss of mitochondrial membrane potential (Fig. 9). In combination, the data indicate that Bid cleavage and subsequent triggering of mitochondrial apoptosis is critical for sensitivity of the cells to low levels of Pc 181-PDT. Other mechanisms, including direct mitochondrial photodamage, may bypass the absence of Bid at higher levels of Pc 181-PDT. Furthermore, the kinetics of Bid cleavage (Fig. 7) and cytochrome c release (Fig. 6E) are consistent with a critical role of Bid cleavage in the triggering of PDT-induced apoptosis, as previously found for other lysosome-targeting photosensitizers (7,13).

The close correlation between the levels of cell survival (Fig. 4) and apoptosis (e.g., Fig. 5D) suggests that PDT with Pc 181 kills cells, whether Bid$^{+/+}$ or Bid$^{-/-}$, mainly by apoptosis. The release of cytochrome c from mitochondria, an early step in the mitochondrial pathway of apoptosis, not only triggers caspase activation necessary for the execution of apoptosis, but also may disrupt mitochondrial respiration and energy production leading to mitochondrial dysfunction and cell death (25). Indeed, dissipation of the mitochondrial membrane potential was more severe in Bid$^{+/+}$ than in Bid$^{-/-}$ MEFs following Pc 181-PDT (Fig. 9). Furthermore, both Bid cleavage (Fig. 7A) and cytochrome c release (Fig. 6E) begin as early as 1 h after PDT with 100 nM Pc 181, whereas the loss of mitochondrial membrane potential (Fig. 9A) overlaps in time with these events. At 50 nM Pc 181, Bid cleavage also begins by 1 h after PDT (Fig. 7A) and clearly precedes cytochrome c release, which is not greater than the control level until 3 h after PDT (Fig. 6E). Previous studies (7,30) have found that the loss of mitochondrial membrane potential in response to PDT-induced lysosome damage follows Bid cleavage, cytochrome c release, and caspase activation. Our data are consistent with that general time course.

Despite inhibition of mitochondrial apoptosis in the absence of Bid following low doses of PDT with Pc 181, apoptosis still occurs in Bid$^{-/-}$ cells after higher doses of PDT, although at lower levels than that found in Bid$^{+/+}$ cells. The induction of apoptosis in the absence of Bid may result from either a non-specific accumulation of Pc 181 in other subcellular compartments or through activation of a Bid-independent pathway of apoptosis at higher doses of PDT. The former possibility is supported by the findings of Ichinose et al. (12) and our laboratory (14) that Bcl-2, which is destroyed effectively by mitochondrion/ER-targeted PDT, such as with Pc 4, can also be photodamaged by PDT with the lysosome-specific photosensitizers, ATX-s10 and Pc 181.

Lysosomes contain hydrolytic proteases that are responsible for the recycling of cellular organelles and macromolecules (26) through processes termed macro- or micro-autophagy (27). The hydrolytic proteases of the cathepsin family not only function in general protein turnover, they also have other functions outside the lysosomal compartment (28). For example, in cancer cells cathepsins are secreted into the extracellular space and can enhance cellular mobility, invasion, and angiogenesis. Of greater relevance to the present study, cathepsins when released into the cytoplasm participate in the cell death process both via classic apoptosis mediated by cleavage of Bid (discussed above) and via programmed cell

death mechanisms that are caspase- and mitochondrion-independent (29). Cancer cells, however, have altered lysosomal properties that render them more susceptible than normal cells to therapies that target lysosomes (28). These include an enhanced expression of cysteine cathepsins, enhanced sensitivity of lysosomal membranes to programmed cell death-inducing stimuli, increased volume and number of lysosomes, and altered trafficking of lysosomes. Since Pc 181-PDT has been found to be more effective in cell killing than mitochondrion-targeting Pc 4-PDT in a previous study of MCF-7c3 cells (14) and at least as effective in the present study, our PDT data support a role for lysosomes as good targets for therapy. Pc 181-PDT was 4–6 times more efficient in killing MCF-7c3 cells than was Pc 4-PDT (14), whereas there is no more than a two-fold difference in the effectiveness of the two photosensitizers in MEFs. We do not know the reason for the very small differential sensitivity of MEFs to Pc 4 vs. Pc 181, but we speculate that at least part of the reason is a difference in the importance of lysosomal vs. mitochondrial/ER damage in triggering cell death. Because the one condition that shows greater phototoxicity in MEFs than all the rest is the use of Pc 181 in the Bid$^{+/+}$ cells, the lysosome pathway must be responsible for that added photosensitivity. In MCF-7 cells, the lysosome pathway may have even greater importance, and if that is the case, it may explain the 4–6-fold greater activity of Pc 181 than Pc 4 in those cells.

Acknowledgments

References

1. Moan J, Berg K. Photochemotherapy of cancer: experimental research. Photochem. Photobiol. 1992; 55:931–948. [PubMed: 1409894]

2. Weishaupt KR, Gomer CJ, Dougherty TJ. Identification of singlet oxygen as the cytotoxic agent in photoinactivation of a murine tumor. Cancer Res. 1976; 36:2326–2329. [PubMed: 1277137]

3. Peng Q, Moan J, Nesland JM. Correlation of subcellular and intratumoral photosensitizer localization with ultrastructural features after photodynamic therapy. Ultrastruct Pathol. 1996; 20:109–129. [PubMed: 8882357]

4. Oleinick NL, Morris RL, Belichenko I. The role of apoptosis in response to photodynamic therapy: what, where, why, and how. Photochem. Photobiol Sci. 2002; 1:1–21. [PubMed: 12659143]

5. Kessel D. Death pathways associated with photodynamic therapy. Med. Laser Appl. 2006; 21:219–224. [PubMed: 19890442]

6. Kessel D, Luo Y, Mathieu P, Reiners JJ Jr. Determinants of the apoptotic response to lysosomal photodamage. Photochem Photobiol. 2000; 71:196–200. [PubMed: 10687394]

7. Reiners JJ Jr, Caruso JA, Mathieu P, Chelladurai B, Yin XM, Kessel D. Release of cytochrome c and activation of pro-caspase-9 following lysosomal photodamage involves Bid cleavage. Cell Death Differ. 2002; 9:934–944. [PubMed: 12181744]

8. Gross A, McDonnell JM, Korsmeyer SJ. BCL-2 family members and the mitochondria in apoptosis. Genes Dev. 1999; 13:1899–1911. [PubMed: 10444588]

9. Wang K, Yin XM, Chao DT, Milliman CL, Korsmeyer SJ. BID: a novel BH3 domain-only death agonist. Genes Dev. 1996; 10:2859–2869. [PubMed: 8918887]

10. Shimizu S, Tsujimoto Y. Proapoptotic BH3-only Bcl-2 family members induce cytochrome c release, but not mitochondrial membrane potential loss, and do not directly modulate voltage-dependent anion channel activity. Proc. Natl. Acad. Sci. USA. 2000; 97:577–582. [PubMed: 10639121]

11. Stoka V, Turk B, Schendel SL, Kim TH, Cirman T, Snipas SJ, Ellerby LM, Bredesen D, Freeze H, Abrahamson M, Bromme D, Krajewski S, Reed JC, Yin XM, Turk V, Salvesen GS. Lysosomal

protease pathways to apoptosis. Cleavage of bid, not pro-caspases, is the most likely route. J. Biol Chem. 2001; 276:3149–3157. [PubMed: 11073962]

12. Ichinose S, Usuda J, Hirata T, Inoue T, Ohtani K, Maehara S, Kubota M, Imai K, Tsunoda Y, Kuroiwa Y, Yamada K, Tsutsui H, Furukawa K, Okunaka T, Oleinick NL, Kato H. Lysosomal cathepsin initiates apoptosis, which is regulated by photodamage to Bcl-2 at mitochondria in photodynamic therapy using a novel photosensitizer, ATX-s10 (Na). Int. J Oncol. 2006; 29:349–355. [PubMed: 16820876]

13. Wan Q, Liu L, Xing D, Chen Q. Bid is required in NPe6-PDT-induced apoptosis. Photochem Photobiol. 2008; 84:250–257. [PubMed: 18173728]

14. Rodriquez ME, Zhang P, Azizuddin K, Santos GBD, Chiu S, Xue L, Berlin JC, Peng X, Wu H, Lam M, Nieminen A, Kenney ME, Oleinick NL. Structural factors and mechanisms underlying the improved photodynamic cell killing with silicon phthalocyanine photosensitizers directed to lysomes versus mitochondria. Photochem Photobiol. 2009; 85:1189–1200. [PubMed: 19508642]

15. Chiu SM, Oleinick NL. Dissociation of mitochondrial depolarization from cytochrome c release during apoptosis induced by photodynamic therapy. Br. J. Cancer. 2001; 84:1099–1106. [PubMed: 11308261]

16. Xue LY, Chiu SM, Oleinick NL. Photodynamic therapy-induced death of MCF-7 human breast cancer cells: a role for caspase-3 in the late steps of apoptosis but not for the critical lethal event. Exp Cell Res. 2001; 263:145–155. [PubMed: 11161713]

17. Chiu S, Evans HH, Lam M, Nieminen A, Oleinick NL. Phthalocyanine 4 photodynamic therapy-induced apoptosis of mouse L5178Y–R cells results from a delayed but extensive release of cytochrome c from mitochondria. Cancer Lett. 2001; 165:51–58. [PubMed: 11248418]

18. Trivedi NS. Quantitative analysis of Pc 4 localization in mouse lymphoma (LY-R) cells via double-label confocal fluorescence microscopy. Photochem. Photobiol. 2000; 71:634–639. [PubMed: 10818795]

19. Lam M, Oleinick NL, Nieminen AL. Photodynamic therapy-induced apoptosis in epidermoid carcinoma cells. Reactive oxygen species and mitochondrial inner membrane permeabilization. J. Biol. Chem. 2001; 276:47379–47386. [PubMed: 11579101]

20. Usuda J, Chiu SM, Murphy ES, Lam M, Nieminen AL, Oleinick NL. Domain-dependent photodamage to Bcl-2. A membrane anchorage region is needed to form the target of phthalocyanine photosensitization. J. Biol Chem. 2003; 278:2021–2029. [PubMed: 12379660]

21. Chiu SM, Xue LY, Usuda J, Azizuddin K, Oleinick NL. Bax is essential for mitochondrion-mediated apoptosis but not for cell death caused by photodynamic therapy. Br. J. Cancer. 2003; 89:1590–1597. [PubMed: 14562036]

22. Xue LY, Chiu SM, Oleinick NL. Staurosporine-induced death of MCF-7 human breast cancer cells: a distinction between caspase-3-dependent steps of apoptosis and the critical lethal lesions. Exp Cell Res. 2003; 283:135–145. [PubMed: 12581734]

23. Li H, Zhu H, Xu CJ, Yuan J. Cleavage of BID by caspase 8 mediates the mitochondrial damage in the Fas pathway of apoptosis. Cell. 1998; 94:491–501. [PubMed: 9727492]

24. Cirman T, Oresic K, Mazovec GD, Turk V, Reed JC, Myers RM, Salvesen GS, Turk B. Selective disruption of lysosomes in HeLa cells triggers apoptosis mediated by cleavage of Bid by multiple papain-like lysosomal cathepsins. J. Biol Chem. 2004; 279:3578–3587. [PubMed: 14581476]

25. Varnes ME, Chiu SM, Xue LY, Oleinick NL. Photodynamic therapy-induced apoptosis in lymphoma cells: translocation of cytochrome c causes inhibition of respiration as well as caspase activation. Biochem. Biophys. Res Commun. 1999; 255:673–679. [PubMed: 10049769]

26. DeDuve C. Lysosomes revisited. Eur. J Biochem. 1983; 137:391–397. [PubMed: 6319122]

27. Levine B, Klionsky DJ. Development by self-digestion: molecular mechanisms and biological functions of autophagy. Dev. Cell. 2004; 6:463–477. [PubMed: 15068787]

28. Fehrenbacher N, Jaattela M. Lysosomes as targets for cancer therapy. Cancer Res. 2005; 65:2993–2995. [PubMed: 15833821]

29. Jaattela M, Cande C, Kroemer G. Lysosomes and mitochondria in the commitment to apoptosis: a potential role for cathepsin D and AIF. Cell Death Differ. 2004; 11:135–136. [PubMed: 14647234]

30. Caruso JA, Mathieu PA, Joiakim A, Leeson B, Kessel D, Sloane BF, Reiners JJ Jr. Differential susceptibilities of murine hepatoma 1c1c7 and Tao cells to the lysosomal photosensitizer NPe6:

Influence of aryl hydrocarbon receptor on lysosomal fragility and protease contents. Mol. Pharmacol. 2004; 65:1016–1028. [PubMed: 15044632]
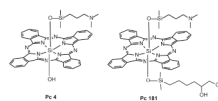
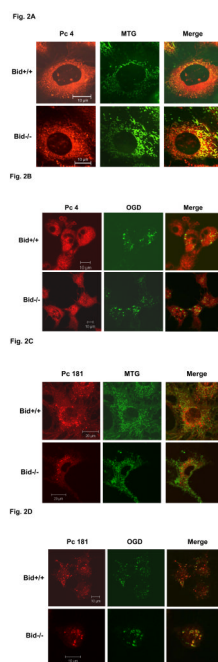**Fig. 1.**
Structures of Pc 4 and Pc 181

Fig. 2.
Localization of Pc 4 and Pc 181 in MEFs. MEFs were cultured in glass-bottom dishes, loaded with either with 200 nM Pc 4 (A, B) or 100 nM Pc 181 (C, D) and incubated at 37° C for 18 h. The cultures were further incubated with either 100 nM MTG (A, C) or 0.2 mg/mL OGD (B, D). They were then viewed by confocal microscopy
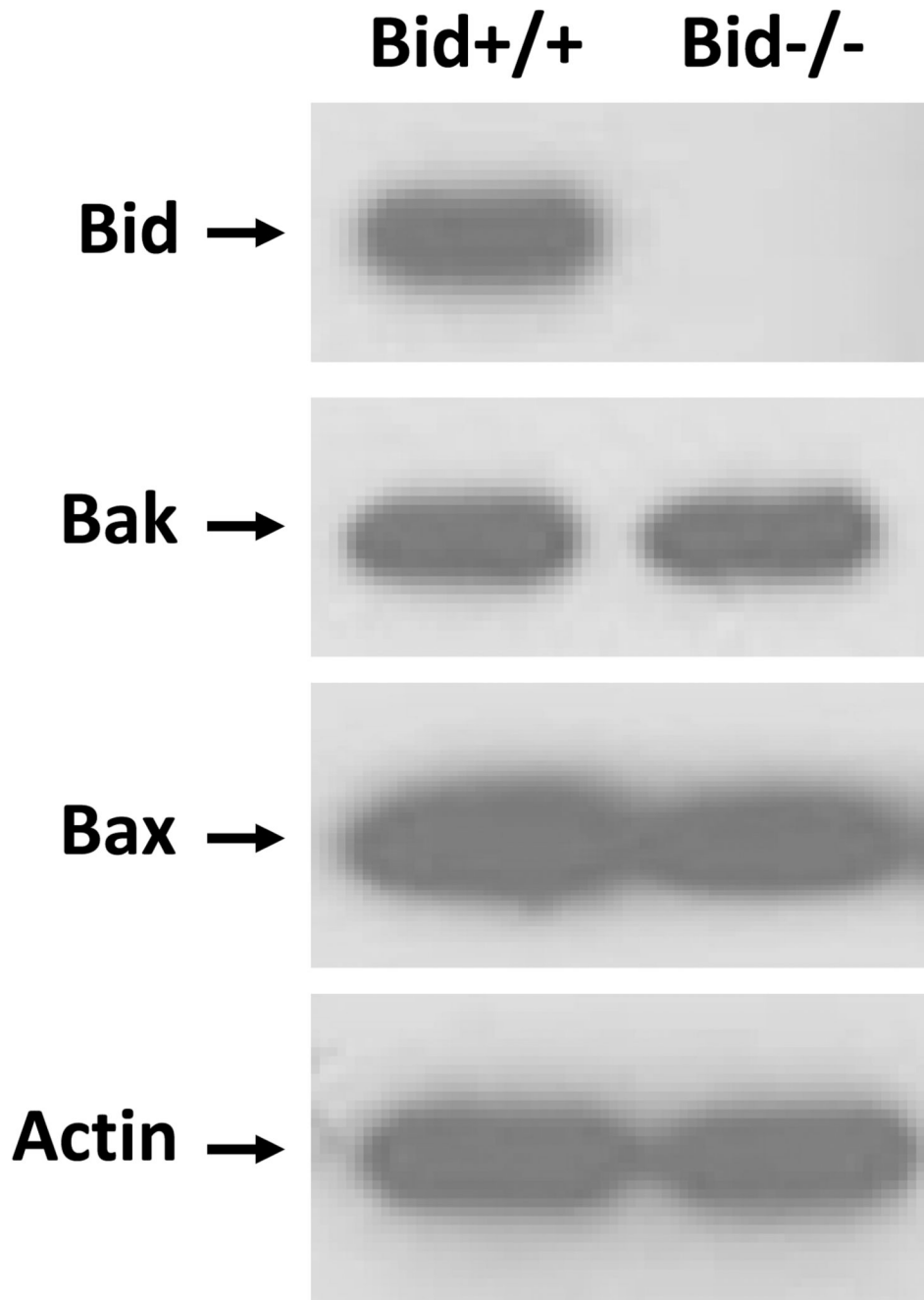
Fig. 3.
Western blot analysis of the expression of Bid, Bax, Bak, and actin (as loading control) in Bid$^{+/+}$ and Bid$^{-/-}$ cells. Equal amounts of protein from whole cell lysates were resolved on SDS-PAGE and processed for western blot analysis
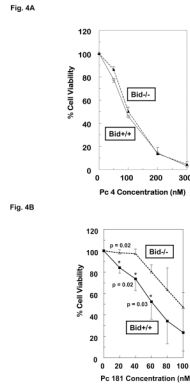
Fig. 4C
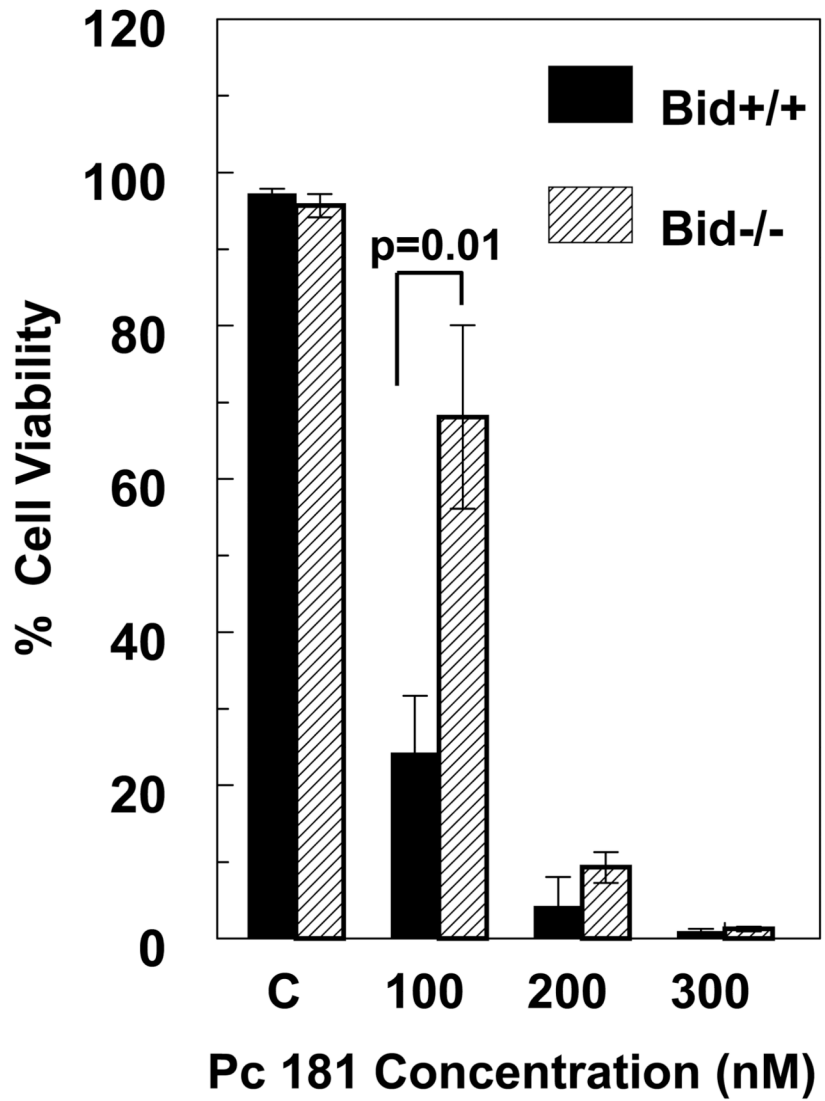
Fig. 4.

Dose dependence of the loss of cell viability. Exponentially growing cultures of Bid$^{+/+}$ or Bid$^{-/-}$ cells in 96-well plates were incubated 6–18 h in either 0–300 nM Pc 4 (A) or 0–100 nM Pc 181 (B). The cultures were irradiated with 200 mJ/cm^2 red light and subjected to MTT assay after 22 h of post-irradiation incubation. Data are the mean ± SD of results of duplicate plates in 3 experiments. (C) Viability of Bid$^{+/+}$ and Bid$^{-/-}$ cells 20 h after Pc 181-PDT (100 nM Pc 181 + 200 mJ/cm^2 red light), as determined by trypan blue exclusion. The data represent the mean ± SD of duplicate measurements on at least 150 cells in each of two experiments

Fig. 5A

Fig. 5B

Fig. 5C

Fig. 5D
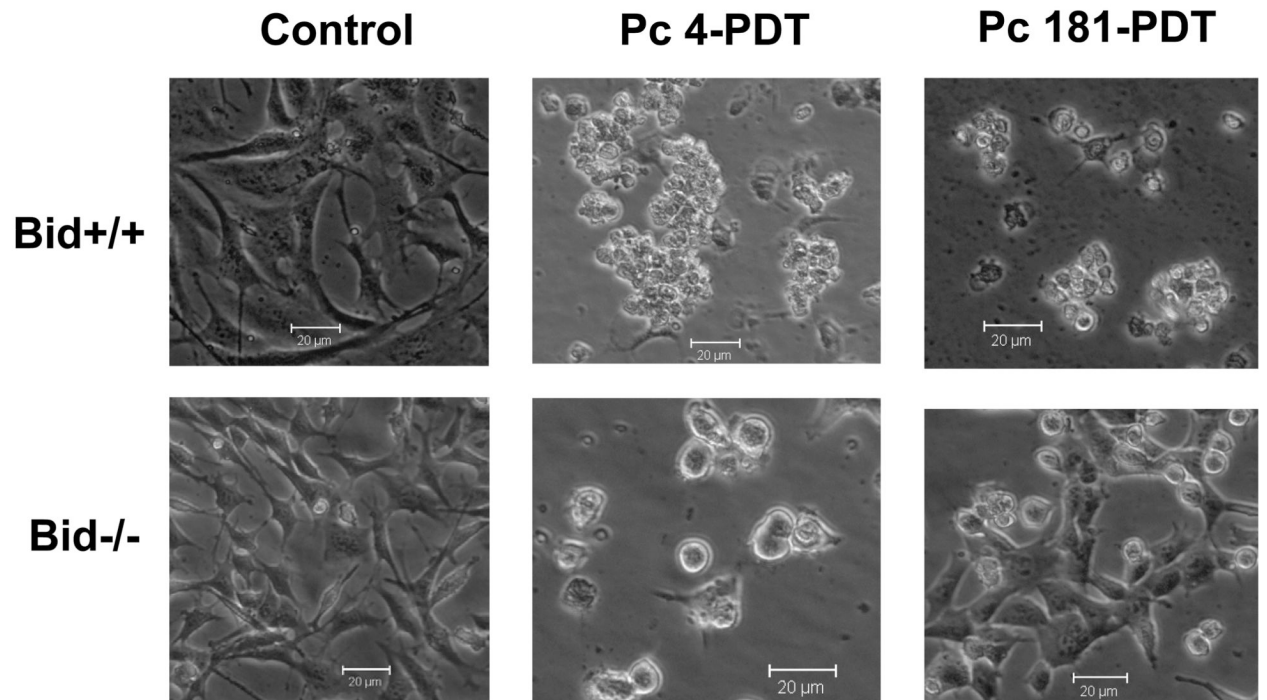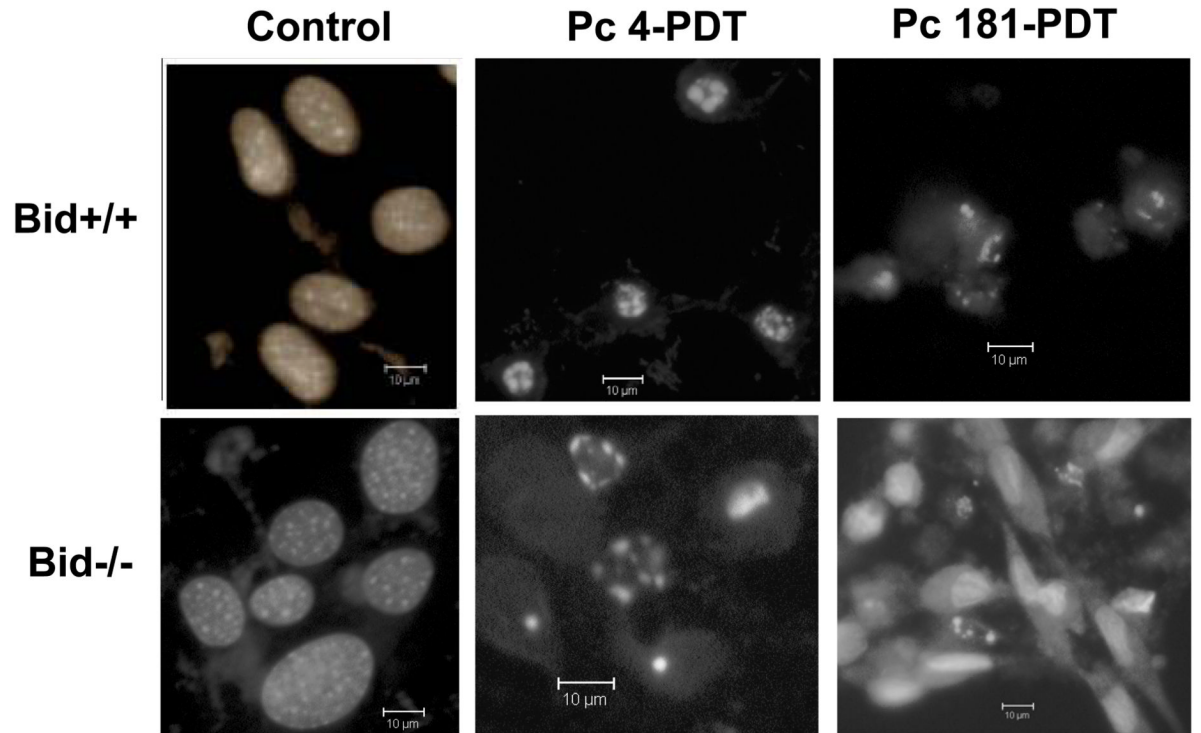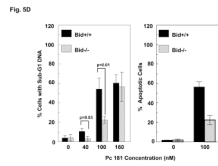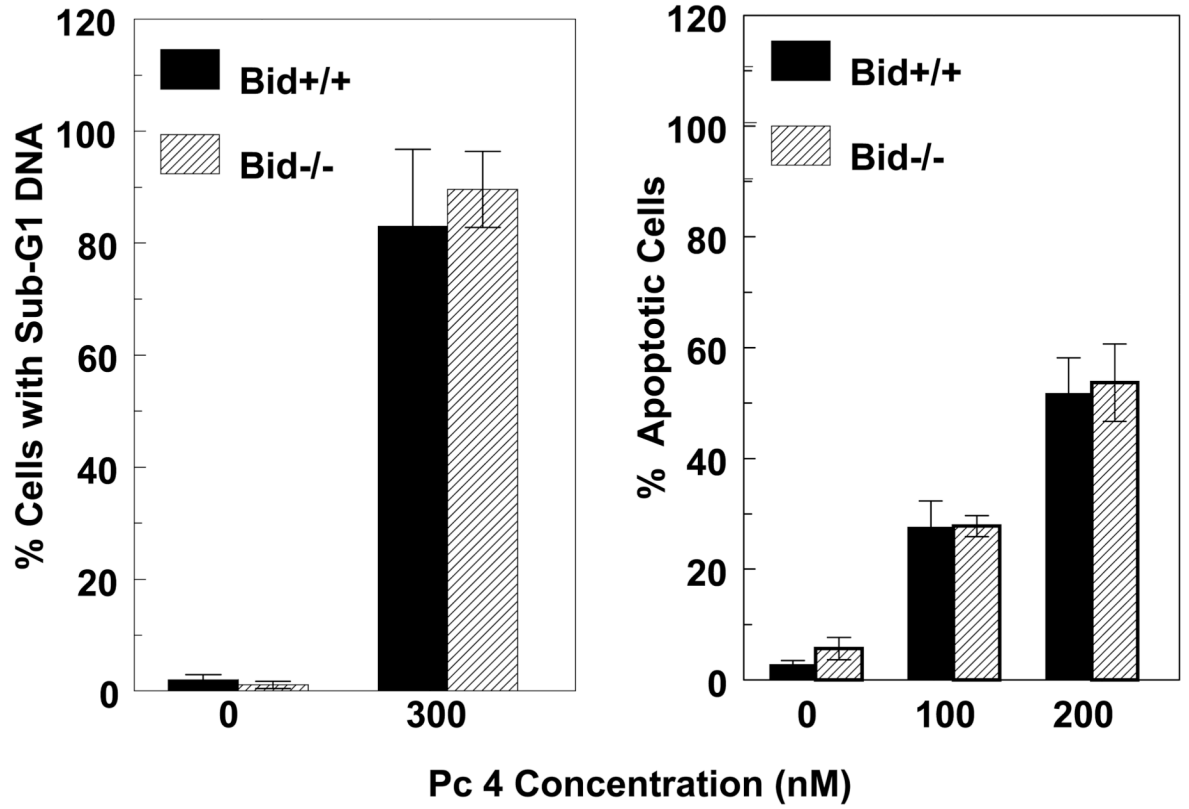
Fig. 5E
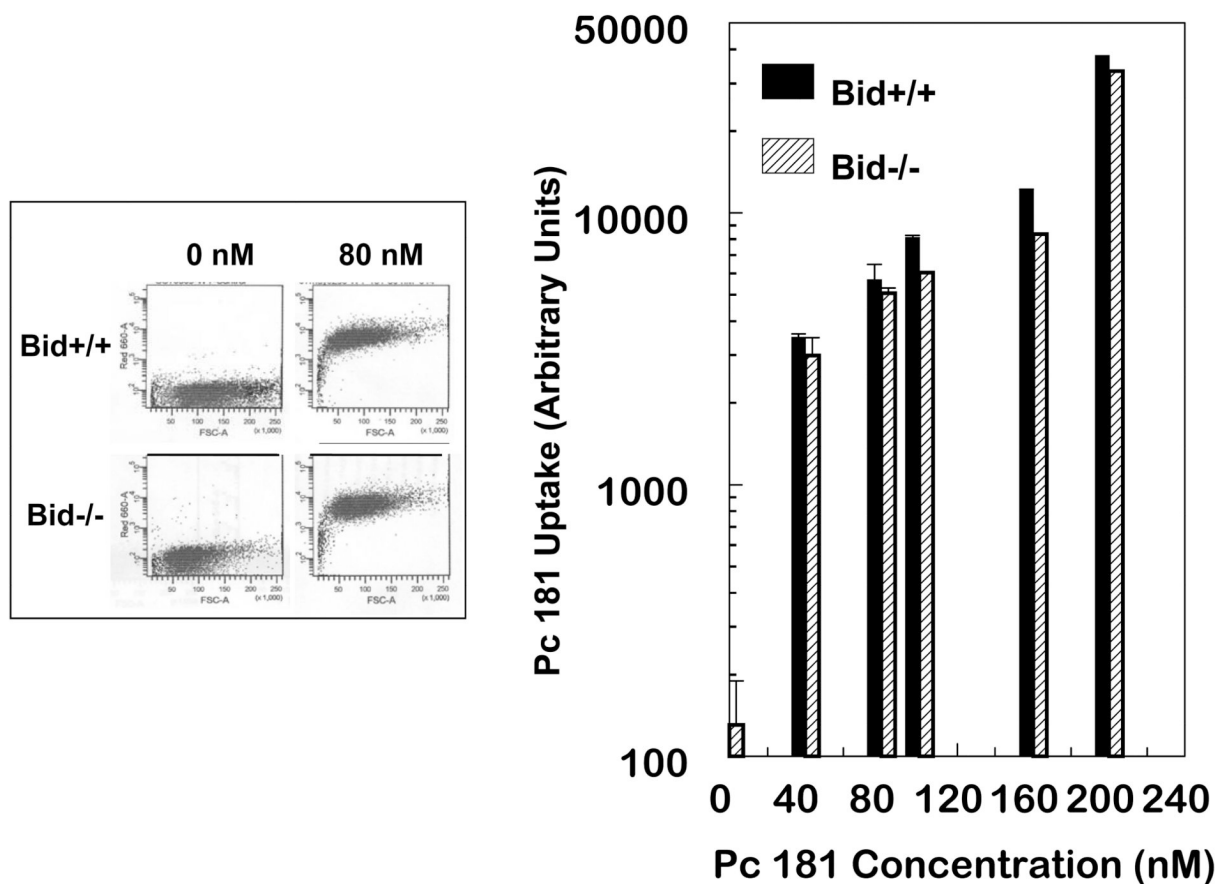
Fig. 5.
Induction of apoptosis by PDT with Pc 4 or Pc 181. (A,B) Change in cell (A) and nuclear (B) morphology after PDT. $Bid^{+/+}$ and $Bid^{-/-}$ MEFs growing in 12-well plates were either untreated or treated with Pc 4-PDT (300 nM Pc 4, 200 mJ/cm^2 red light) or Pc 181 (100 nM Pc 181, 200 mJ/cm^2 red light) followed by 24 h post-irradiation incubation. The nuclear DNA was stained with Hoechst 33342 and examined by fluorescence microscopy. (C,D) Dose dependence for the induction of apoptosis. MEFs were loaded with 0–300 nM Pc 4 (panel C) or 0–160 nM Pc 181 (panel D) for 18 h and then exposed to 200 mJ/cm^2. After 20 h of further incubation, apoptosis was estimated by the percentage of Hoechst 33342-stained nuclei with apoptotic features (right panels) or the percentage of cells with less than the G1 content of DNA (left panels). Data for Hoechst staining represent the mean ± SD from duplicate coverslips for each condition in two independent experiments. Data for sub-G1 DNA content represent the mean percentage of cells with sub-G1 DNA from duplicate cultures in each of three experiments ± SD. (E) Concentration dependence of the uptake of Pc 181 into $Bid^{+/+}$ and $Bid^{-/-}$ MEFs. Exponentially growing cultures were loaded with 0–200 nM Pc 181 for 16–18 h. Cells were collected, washed, and analyzed by flow cytometry
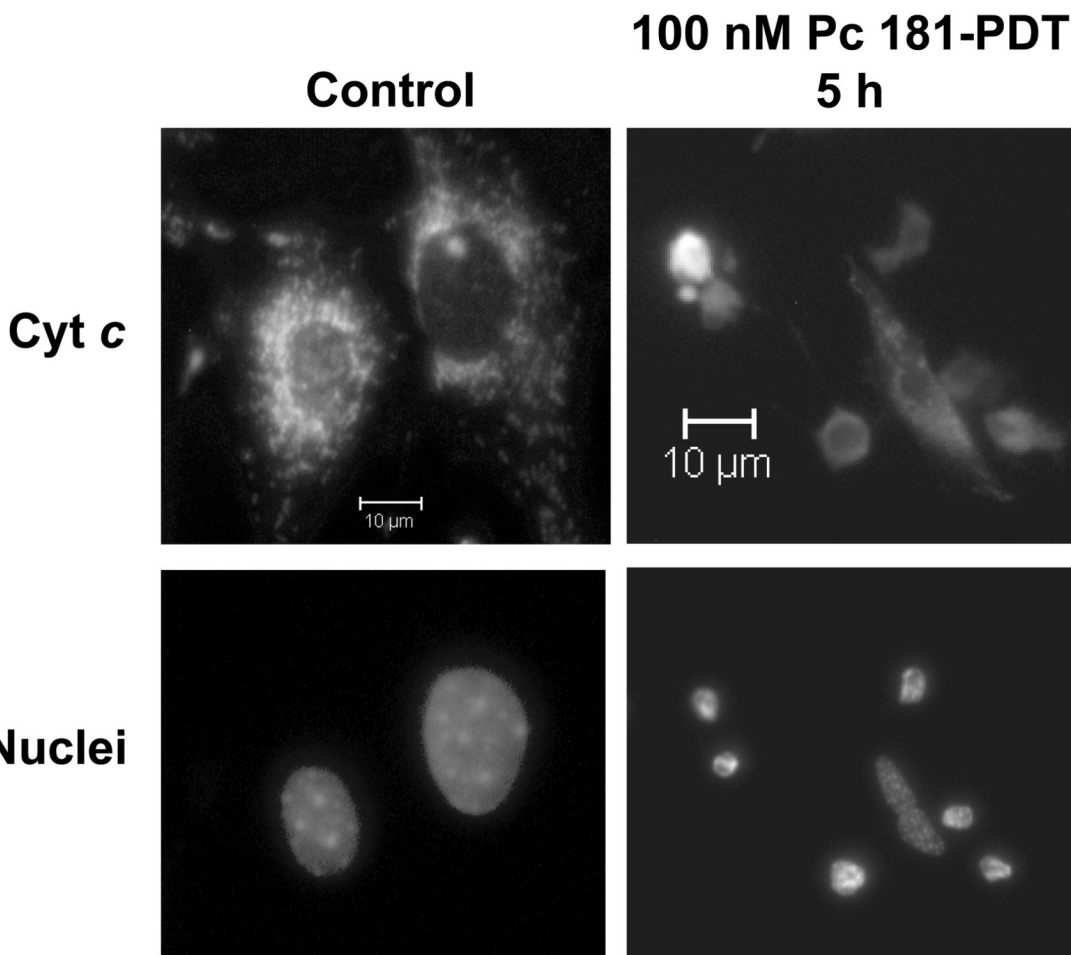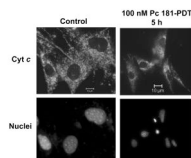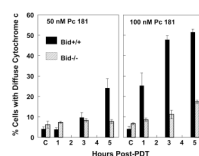
Fig. 6A
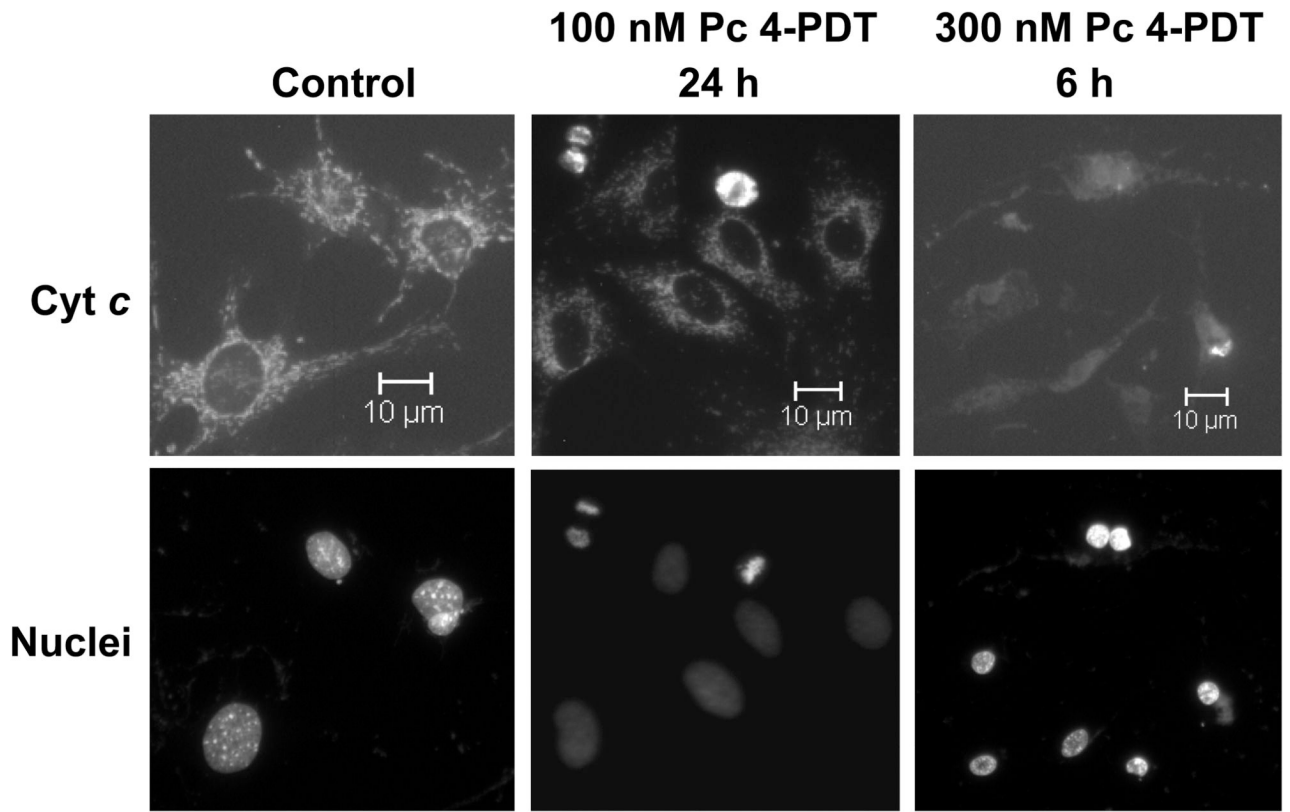
Fig. 6C
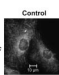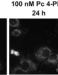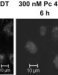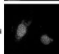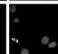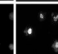
Fig. 6.
Pc 181-PDT fails to induce the release of cytochrome c in Bid$^{-/-}$ cells. MEFs were untreated or treated with either 100–300 nM Pc 4 (A, B) or 100 nM Pc 181 (C, D) plus red light followed by 5–24 h of incubation. The release of cytochrome c from mitochondria was

monitored by fluorescence immunostaining. (A,C) $Bid^{+/+}$, (B,D) $Bid^{-/-}$ cells. Nuclear DNA was stained with Hoechst 33342. (E) Time course for the release of cytochrome c from mitochondria in MEFs following PDT with 50 (left panel) or 100 (right panel) nM Pc 181. The percentage of cells with diffuse cytochrome c was estimated in at least 200 cells on duplicate cover slips such as those in panels C and D. Data represent the mean ± SD from duplicate coverslips for each condition in one (for 50 nM) or two (for 100) independent experiments

Fig. 7A

Fig. 7B
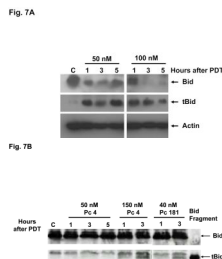
Fig. 7.
Cleavage of Bid following PDT with Pc 4 or Pc 181. Bid$^{+/+}$ MEFs were untreated or exposed to (A) Pc 181-PDT (50 or 100 nM Pc 181, 200 mJ/cm^2) or (B) Pc 4-PDT (50 or 150 nM Pc 4, 200 mJ/cm^2) or Pc 181-PDT (40 nM Pc 181, 200 mJ/cm^2). Cells were collected at 1, 3 and 5 h after PDT, and whole cell lysates were analyzed on western blots
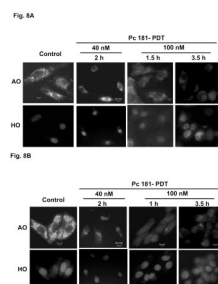
Fig. 8.
Loss of lysosomal integrity in MEFs following Pc 181-PDT. Bid$^{+/+}$ (A) and Bid$^{-/-}$ (B) cells grown on coverslips were either untreated or treated with PDT (40 or 100 nM Pc 181, 200 mJ/cm^2 red light). After various periods of post-irradiation incubation, cultures were loaded with 1µg/mL of acridine orange (AO) and Hoechst 33342 (HO) for 20 min and examined by fluorescence microscopy
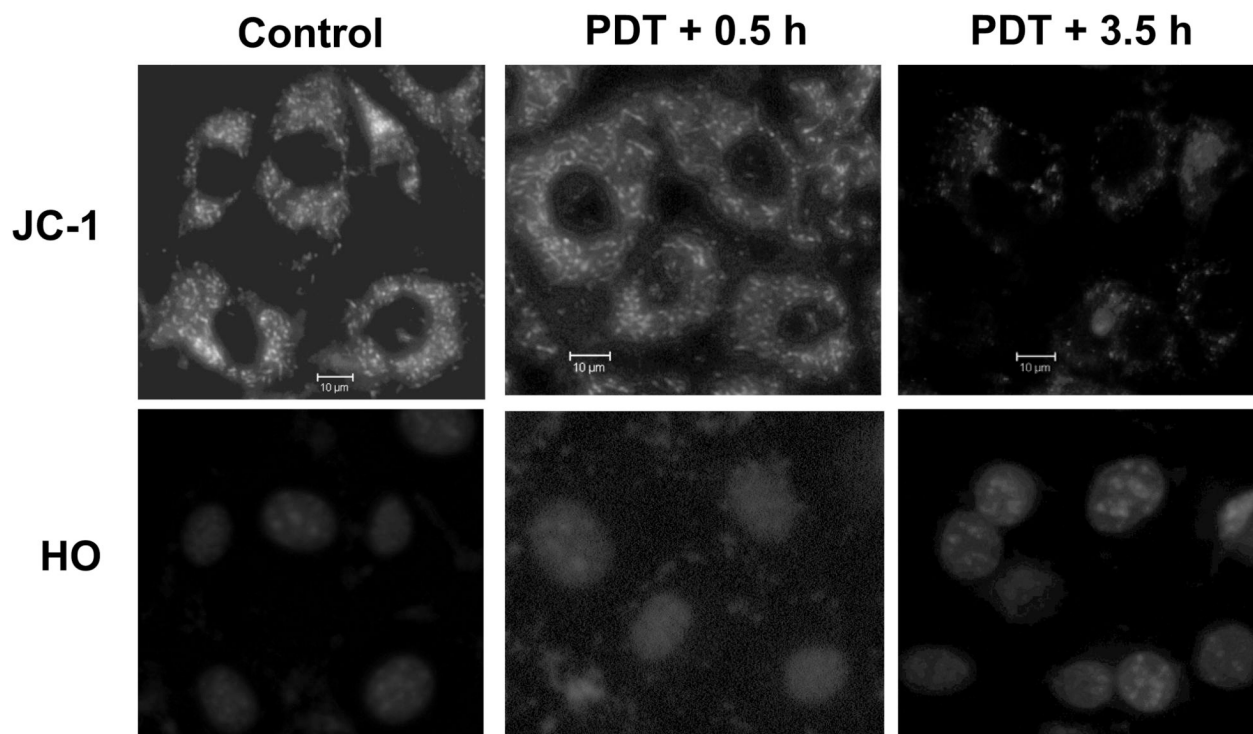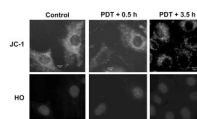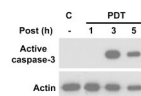
Fig. 9A

Fig. 9.
Loss of mitochondrial membrane potential and release of cytochrome c in MEFs following Pc 181-PDT. Bid$^{+/+}$ (A) and Bid$^{-/-}$ (B) cells were grown and treated with PDT as indicated in Fig. 7 After 0.5 and 3.5 hours post-irradiation incubation, cells were stained with JC-1 and Hoechst 33342 for 30 min and examined by fluorescence microscopy. (C) Bid+/+ cells were evaluated for the activation of caspase-3 by western blotting at various times following PDT with 100 nM Pc 181